α-$K_4R_6I_{14}Os$ (R = La, Pr): A Novel Iodine-Rich Structure with a Layered Network of Electron-Poor Clusters. An Incipient Delocalized System with Metal-like Conductivity

S. Uma, James D. Martin, and John D. Corbett*

Department of Chemistry, Iowa State University, Ames, Iowa 50011

Received June 2, 1999

The title compounds are obtained from reactions of KI, RI_3, R, and Os at 750−850 °C in sealed Nb or Ta containers. The structure was established by single-crystal X-ray diffraction studies (tetragonal, *P*4/*mnc*, $Z = 2$; $a = 10.044(4)$, 9.879(3) Å and $c = 21.825(4)$, 21.86(1) Å for La, Pr, respectively) for three samples, La and Pr at 23 °C and La at −100 °C. This particular combination of large R, interstitial Z, and halogen results in the highest X:R ratio known among rare-earth-metal cluster halides and an unprecedented structure type. The cluster units are interconnected according to the pattern $[(R_6Os)I^i_8I^{i-a}_{4/2}I^{a-i}_{4/2}I^a_2]^{4-}$ in which four R in the waist of each cluster, the Os, and four bridging $I^{i-a,a-i}$ pairs generate a planar 2D network of geometrically nearly ideal, 16-electron R_6Os octahedra. This contrasts with the tetragonal compression found for many other 16-e^- examples with the parallel disappearance of Curie−Weiss paramagnetism. Powdered α-$K_4La_6I_{14}Os$ exhibits an exceptionally low resistivity for a cluster halide (∼120 μΩ·cm) over 110−280 K and a small paramagnetism over about 35 to ∼250 K associated with a probable Mott−Hubbard state that changes to a temperature-independent (presumably Pauli) paramagnetism above about 300 K. EHTB band calculations show that a significant broadening of the HOMO ($\sim t_{1u}$) states takes place in the plane of the intercluster bridging. The unique structure, properties, and band picture for the compound indicate a transition to a delocalized (band) state.

Introduction

Metal cluster chemistry has in the past decade or so provided considerable new information and insights into the many factors important in metal−metal bonding. One remarkable feature has been the discovery that virtually all cluster halides of the early transition metals (groups 3 and 4) require a centered heteroatom (Z) for stability.[1−7] Particularly novel compounds are found among the rare-earth-metal (R) cluster halides (X). The majority of these consist of well-known R_6X_{12} units centered by the requisite Z. The interstitials provide not only central R−Z bonding within the cluster but also additional valence electrons that aid in fulfilling certain minimal electron counts necessary for R−Z and R−R bonding in these relatively electron-poor clusters.[8] Workable interstitial atoms include the late transition metals (groups 7−11), lighter main-group elements (Be−N, Si, etc.), and even C_2 dimers.[9,10] The clusters may be either isolated from each other by bridging halides or condensed into dimers, tetramers, or infinite chains, depending essentially upon the X:R ratio.

Although this kind of chemistry is already distinctive and extensive, numerous new and novel structures are still found through exploratory synthesis guided by electronic and structural principles. Recent achievements in the quaternary A−R−I−Z systems (A = alkali metal) have been especially noteworthy. The earliest examples contained main-group interstitials in such clusters as $Cs_4Pr_6I_{13}C_2$, $Cs_4Sc_6I_{13}C$,[9] $Cs_2Pr_6I_{12}C_2$,[10] and $CsEr_6I_{12}C$.[11] Only four structure types have been described for transition-metal-stabilized examples: (a) $Cs_4R_6I_{13}Z$ (R = Ce, Pr; Z = Co, Os),[3] which exhibit a novel interconnection pattern between the clusters and halides, $Cs_4(R_6Z)I^i_8I^{i-a}_{4/2}I^{a-i}_{4/2}I^{a-a}_{2/2}$ (where I^i is edge-bridging on the clusters, I^a is exo at a vertex, and the combinations represent dual functions), (b) the composition $AR_6I_{10}Z$ (A = K, Cs; R = La, Pr; Z = Mn, Fe, Os),[4] which with fewer halides exhibits a greater degree of intercluster connectivity; (c) bioctahedral clusters in $A_2R_{10}I_{17}Z_2$ (A = Rb, Cs; R = La, Ce, Pr; Z = Co, Ni, Ru, Os),[5,6] in which edge-sharing cluster $R_{10}Z_2$ units are sheathed and interbridged by iodine atoms; (d) the latest $K_2La_6I_{12}Os$ type,[7] in which strained I^{i-a} and I^{a-i} bridges link tetragonally compressed 16-e^- closed-shell (diamagnetic) $La_6(Os)I_{12}$ clusters. Our more recent emphases have been on La (Y or Sc) cluster systems in order to avoid the paramagnetic $4f^n$ centers, which obscure the more subtle information that can be obtained from magnetic susceptibility data for examples that deviate from the ideal 18 cluster-based electrons.

Synthetic experiments still seem to be the only route to new phases in these areas. The present work describes exactly such an instance in which an unprecedented network design provides what appears to be an ideal connectivity for intercluster electron delocalization. And, in contrast to previous 16-e^- cluster

(1) (a) Corbett, J. D. In *Modern Perspectives in Inorganic Crystal Chemistry*; Parth, E., Ed.; Kluwer Academic Publishers: Dordrecht, The Netherlands, 1992; p 27. (b) Corbett, J. D. *J. Alloys Compd.* **1995**, *224*, 10.
(2) Simon, A.; Mattausch, H.; Miller, G. J.; Bauhofer, W.; Kremer, R. K. In *Handbook on the Physics and Chemistry of Rare Earths*; Gschneider, K. A., Jr., Eyring, L., Eds.; Elsevier Science Publishers B.V.: Amsterdam, 1991; Vol. 15, p 191.
(3) Lulei, M.; Corbett, J. D. *Inorg. Chem.* **1996**, *35*, 4084.
(4) Lulei, M.; Corbett, J. D. *Z. Anorg. Allg. Chem.* **1996**, *622*, 1677.
(5) Lulei, M.; Maggard, P. A.; Corbett, J. D. *Angew. Chem., Int. Ed. Engl.* **1996**, *35*, 1704.
(6) Lulei, M.; Martin, J. D.; Hoistad, L. M.; Corbett, J. D. *J. Am. Chem. Soc.* **1997**, *119*, 513.
(7) Uma, S.; Corbett, J. D. *Inorg. Chem.* **1998**, *37*, 1944.
(8) Hughbanks, T. *Prog. Solid State Chem.* **1989**, *19*, 329.
(9) Artelt, H. M.; Meyer, G. *Z. Anorg. Allg. Chem.* **1994**, *620*, 1521.
(10) Artelt, H. M.; Meyer, G. *Z. Anorg. Allg. Chem.* **1993**, *619*, 1.
(11) Artelt, H. M.; Schleid, T.; Meyer, G. *Z. Anorg. Allg. Chem.* **1992**, *618*, 18.

10.1021/ic990638f CCC: $18.00
Published on Web 08/05/1999

structures that show tetragonal compression, these units with expected $\sim t_{1u}^4$ HOMO configurations are undistorted. During the present investigation, we also discovered a second very different polytype of $K_4La_6I_{14}Os$ [$=(K_4I)La_6I_{13}Os$],[12] so the present phase is designated as the α-form.

Experimental Section

Synthesis. All reactions utilized rare-earth metals R = La, Pr, their triiodides RI_3, NaI, KI or K, RbI or CsI, and transition elements Z. The R metals (Ames Laboratory, 99.99%), potassium (Baker, 99.9%, under Ar), and the transition metals Mn, Fe, Ru, and Os (Alfa, 99.95%) were used as received. The alkali-metal iodides (Fisher, 99.95%) were dried under dynamic vacuum and then sublimed. All operations were carried out in N_2-filled gloveboxes because of the air and moisture sensitivity of some reagents and all of the products. The general reaction techniques in welded Nb or Ta tubing were as previously described.[3−7]

(α-)$K_4La_6I_{14}Os$ was initially observed as a minor product (along with La_2IOs_2[13] and KI) from a reaction mixture loaded as $K_2La_4I_5Os$ that had been heated at 850 °C for 4 weeks and slowly cooled (5 °C/h) to 300 °C. The yield was ∼20% according to a comparison of the relative scattering intensities in the Guinier powder diffraction pattern with that calculated after the structure had been determined. Initially, reactions carried out with the indicated stoichiometry $K_4La_6I_{14}Os$ at 750−850 °C for 28 days did not yield the desired compound, but rather another new phase, β-$K_4La_6I_{14}Os$.[12] Several reactions were run with variations in the amount of K and I, and those with a slightly reduced iodine proportion, e.g., $K_4La_6I_{12}Os$, often resulted in higher yields of α-$K_4La_6I_{14}Os$ (∼85% plus ca. 10% LaOI, a common impurity that probably arises from moisture evolved from the silica jacket on heating and which serves to increase the remaining I:R ratio). The phase was also obtained in ∼75% yield (with 25% LaOI) from the composition $K_4La_6I_{13}Os$ and in 70% yield from the loaded composition $K_6La_6I_{14}Os$ (together with 15% LaOI plus 15% KI). Systems with the ideal composition were also encounted in which the α- and β-forms were in apparent equilibrium, ∼40% each plus 20% LaOI, after reaction for 21 days at 910 °C. Several other reactions run with Fe, Ru, and Ir as potential interstitials gave unidentified products, while Mn and Re were not incorporated. Reactions with Na instead of K resulted in major amounts of the new $NaLa_6I_{12}Os$ (plus ∼10% NaI), while Rb resulted in yet another unknown phase[14] and cesium gave $Cs_4La_6I_{13}Os$, isostructural with $Cs_4R_6I_{13}Z$ (R = Pr, Ce; Z = Co, Os).[3] Stoichiometric praseodymium reactions resulted in a 40% yield of the isostructural $K_4Pr_6I_{14}Os$ along with 20% cubic PrI_2, 25% rhombohedral PrI_2,[15] and powder pattern lines for an unidentified phase or phases.

Single-Crystal X-ray Studies. Small rectangular plates of α-$K_4La_6I_{14}Os$ from different reactions were sealed in thin-walled glass capillaries in the glovebox, and the singularity of each was checked by Laue photographs on Weissenberg cameras. Tetragonal cell parameters and the orientation matrix were obtained from an approximately 0.05 × 0.04 × 0.03 mm crystal via a least-squares refinement of the setting angles of 25 centered reflections collected on a Rigaku AFC6R diffractometer operating with graphite-monochromated Mo Kα radiation. A total of 8000 reflections were collected ($4 \le 2\theta \le 50$ °; $\pm h, \pm k, l$; $2\theta-\omega$ scans) at room temperature. These gave 1225 unique data of which 367 were observed ($I > 3\sigma_I$). ($R_{INT}(F^2) = 39.5\%$ for all reflections; $R_{ave}(F) = 14.92\%$ for 2918 total reflections with $I > 5\sigma_I$). The observation of all orders of *hkl* and *hk*0 reflections along with the absences of *hhl*, $l \neq 2n$, and 0*kl*, $k + l \neq 2n$, supported the choice of space group *P*4/*mnc* (No. 128) or the acentric *P*4/*nc*, and the former was subsequently confirmed by the structure solution and refinement.

The structure was solved by direct methods (SHELXS[16]). Refinement programs, scattering factors, etc. were those in the TEXSAN package.[17] An empirical absorption correction ($\mu = 186.9$ cm^{-1}) was first applied to the full data set with the aid of three ψ scans at χ near 90° and later, after isotropic refinement, by DIFABS as recommended[18] (relative transmission coefficient range: 0.790−1.00). The latter step resulted in a modest reduction of the residuals (from $R(F)/R_w = 0.090/0.101$ to 0.082/0.093, respectively, for 19 variables and 1518 unaveraged reflections), but consistent reductions in the standard deviations, especially for the positional and thermal parameters of lanthanum and iodine. At this stage, the single potassium located on a 2-fold axis along $x, x + {}^1/_2, {}^1/_4$ exhibited a large U_{iso} value, $\sim 14 \times 10^{-2}$ Å^2. This further exhibited an extreme anisotropy, but the position still refined to a 90-(5)% K occupancy. The asymmetry was fully consistent with the electron density distribution synthesized in a Fourier map, which showed two separate maxima normal to the axis. The indicated split (disordered) position refined isotropically to two sites 0.90 Å apart with 47(1)% occupancies, close enough to each other that an anisotropic refinement yielded only extreme and uninformative results. Therefore, only the isotropic refinement of K is reported.

The structure was also carefully refined in the equivalent acentric space group *P*4/*nc*, which lacks this 2-fold axis, to test whether the K disorder was intrinsic or had been induced by use of too-high a symmetry. The former clearly appeared to be the case. The acentric structure was built up from the beginning, first with a direct methods solution for nine atoms and then by successive Δ*F* and minimal refinement steps. The Fourier map after isotropic convergence still showed the two K positions at equal intensity without significant changes in the cluster dimensions. Correlation coefficients in this process were as large as 0.9 between parameters of atoms that would be equivalent in the centric model. The split K positions are entirely consistent with the elongated cavity afforded by the iodine neighbors (below).

The final refinement of all atoms in the centric *P*4/*mnc* with split isotropic K (35 variables, 367 independent reflections) yielded $R(F)/R_w = 0.046/0.034$. The largest residual peak, 3.4 e/Å^3, was at 0.500, 0.478, 0.568. (Refinements of data sets obtained from two other crystals yielded residual peaks of 2.86 and 1.88 e/Å^3 at 1.58 and 1.34 Å from Os, respectively.) Quite comparable results were also obtained from refinement of the isostructural $K_4Pr_6I_{14}Os$. Neither thermal ellipsoid sizes nor occupancy refinements of the heavy atoms in all refinements showed any evidence of significant fractional occupancies.

A data set was also collected from a different crystal at 23 and −100 °C on a CAD4 instrument. The diffractometer lattice constants were also refined at 25 °C intervals between room temperature and −100 °C. These showed about 0.4 and 0.5% contractions in *a* and *c* over the range but no clear irregularities at the 3σ level. More importantly, there was no change in the space group symmetry at −100 °C, and the refined atomic positions were only somewhat more precise and the ellipsoids somewhat smaller than obtained with room-temperature data. Potassium was refined anisotropically on the 2-fold axis, where it gave an occupancy of 94(2)%. The largest residual, 3.6 e/Å^3, was at 0.50, 0.48, 0.47, as above. Other peaks of this size disappeared on correction with DIFABS. The dimensions of the La_6Os octahedron at −100 °C were unchanged at the 1σ level (≤0.004 Å), while most of the La−I distances (except that to I3[a]) had decreased 0.015−0.020 Å.

The Guinier powder pattern calculated for the refined structural model agreed very well with that observed for the bulk product. This allowed indexing of the pattern and, with Si as an internal standard, a better determination of the lattice constants, which were then used in the distance calculations. Some data collection and refinement parameters for the lanthanum compound at room temperature are given in Table 1. The final atom coordinates, isotropic equivalent temperature factors, and their estimated standard deviations are listed in Table 2. Additional data collection and refinement information, the anisotropic displacement parameters for the structure reported here, and all of the corresponding results for $K_4Pr_6I_{14}Os$ and for $K_4La_6I_{14}Os$ at −100 °C are available as Supporting Information. These, the structure factor data, and other information are available from J.D.C.

(12) Uma, S.; Corbett, J. D. *Inorg. Chem.* **1999**, *38*, 3831.
(13) Park, Y.; Martin, J. D.; Corbett, J. D. *J. Solid State Chem.* **1997**, *129*, 277.
(14) Uma, S.; Corbett, J. D. Unpublished research.
(15) Warkentin, E.; Bärninghausen, H. *Z. Anorg. Allg. Chem.* **1979**, *459*, 187.
(16) Sheldrick, G. M. *SHELXS-86*; Universitat Göttingen: Göttingen, Germany, 1986.
(17) *TEXSAN*, Version 6.0; Molecular Structure Corp.: The Woodlands, TX, 1990.
(18) Walker, N.; Stuart, D. *Acta Crystallogr.* **1983**, *A39*, 159.

Table 1. Crystallographic Data for α-$K_4La_6I_{14}Os$[a]

fw	2956.69	V (Å)^3	2202(1)
space group; Z	$P4/mnc$ (No. 128); 2	d_{calc} (g/cm^3)	4.459
lattice constants (Å)		μ(Mo Kα)	186.91
a	10.044(4)	(cm^{-1})	
c	21.825(4)	R, R_w[b]	0.046, 0.034

[a] Cell constants were refined from Guinier powder pattern data measured with Si as an internal standard; λ = 1.540 562 Å; 23 °C. [b] $R = \Sigma||F_o| - |F_c||/\Sigma|F_o|$; $R_w = [\Sigma w(|F_o| - |F_c|)^2/\Sigma w(F_o)^2]^{1/2}$; $w = \sigma_F^{-2}$.

Table 2. Positional and Isotropic Equivalent Displacement Parameters (Å^2) for α-$K_4La_6I_{14}Os$

	Wyckoff					
atom	posn	site sym	x	y	z	B_{eq}[a]
Os	1*a*	4/*m*	0	0	0	1.6(1)
La1	4*e*	4	0	0	0.1310(2)	2.3(1)
La2	8*h*	*m*	0.2703(2)	0.0894(3)	0	2.3(1)
I1	16*i*	1	0.3082(2)	0.1043(3)	0.1488(1)	3.7(1)
I2	8*h*	*m*	0.2051(3)	0.4079(3)	0	4.6(2)
I3	4*e*	4	0	0	0.2824(3)	5.9(2)
K[b]	16*i*	1	0.678(2)	0.143(2)	0.267(1)	5.2(5)

[a] $B_{eq} = (8\pi^2/3)\sum_i\sum_j U_{ij}a_i^*a_j^*\vec{a}_i\vec{a}_j$. [b] Split atom (50:50).

Physical Property Measurements. Magnetic susceptibility measurements were performed on a Quantum Design MSDS SQUID magnetometer for six different 18−30 mg samples from four syntheses of α-$K_4La_6I_{14}Os$, all of which contained only LaOI (and, occasionally, KI) as another component according to their Guinier patterns. These were loaded in a He-filled glovebox into an improved fused-silica container.[19] Magnetizations of the samples at 50 and 100 K were first checked as a function of the applied field (0−6 T) to screen for possible magnetic impurities, but these plots were found to be ideal ($M(T) \rightarrow 0$ at $H \rightarrow 0$). The magnetic susceptibilities were measured at 0.25 and 3 T from 6 to 300 or 400 K. The data were corrected for the susceptibility of the container and with the standard diamagnetic core terms. Unique fits by the generalized nonlinear Curie−Weiss expression $(\chi - \chi_0)^{-1} = (T - \Theta)/C$ were obtained by least-squares means over the whole temperature range to show that the flattening of χ above ~300 K was real, not an artifact of the choice of χ_0. Subsequent plots of $(\chi - \chi_0)^{-1}T$ vs T made it clear that there was also an antiferromagnetic-like transition near ~30−35 K.

Resistivities of two different powdered and sized samples of ~30 mg of $K_4La_6I_{14}Os$ diluted with Al_2O_3 were measured over the range 110−280 K with a high-frequency "Q" apparatus operating at 35 MHz. This method generally gives resistivity values correct within a factor of 2 but good temperature dependencies.

Band Calculations. Calculations[20] were carried out both on the isolated $La_6(Os)I_{18}^{8-}$ cluster with all exo-bonded iodine atoms included and on the full 2D layered lattice of $[La_6I_{14}Os]^{4-}$ at 20 k-points. Charge-iterated H_{ii} parameters used were as follows (in eV). La: 6s, −6.82; 6p, −4.58; 5d, −7.83. Os: 6s, −6.11; 6p, −2.30; 5d, −7.97. I: 5s, −18.00; 5p, −12.7.[6,13,21] Use of values from the density functional theory[22] did not change the results significantly.

Results and Discussion

Synthesis. Explorations for new phases among rare-earth-metal cluster halides require consideration not only the particular metal, halide, interstitial, and countercation involved but also of other structures and compositions that may incorporate the same elements. The consequences of a multiplicity of phases have been particularly noticed in the ternary Y−I−Ru[23] and Pr−I−Ru[13,24] systems. In the present case, there exists a critical region of phase stability such that α-$K_4La_6I_{14}Os$ can be obtained in higher yield from nominally somewhat iodine-poor compositions, i.e., for $K_4La_6I_xOs$, $12 \le x \le 13$ (Experimental Section: Synthesis). (Of course, the usual collateral formation of the usual LaOI in the course of the reaction raises the effective value of x.) Reactions in the same temperature region with the exact stoichiometry often yielded only, or a mixture with, another phase that has been subsequently identified as a second, unrelated tetragonal (β) $K_4La_6I_{14}Os$ type [≙$(K_4I)La_6I_{13}Os$] (space group $P4/ncc$; a = 13.117(3), c = 25.17(1) Å).[12] The two apparent polymorphs do not seem to be related solely by temperature; rather the preferred formation of the present phase from slightly reduced stoichiometries may mean that a compositional difference pertains, but this must be small and not discernible within the limits possible in X-ray refinements. Experiments to establish the variability of the present structure with respect to the alkali- and transition-metal (Z) components (Experimental Section) showed it to be evidently unique for K and Os.

Table 3. Important Distances (Å) and Angles (deg) in $K_4La_6I_{14}Os$

Os−La1	×2	2.855(5)	K−I1	3.39(2)
Os−La2	×4	2.860(3)	K−I1	3.41(2)
			K−I1	3.59(2)
La1−La2	×4	4.041(4)	K−I1	3.77(2)
La2−La2	×2	4.045(4)		
			K−I3	3.55(2)
La1−I1	×4	3.291(3)	K−K[a]	0.90(4)
La1−I3[a]		3.304(9)		
La2−I1	×2	3.274(3)		
La2−$I2^{i-a}$		3.265(5)	I1−La1−I1	166.4(2)
La2−$I2^{i-a}$		3.264(4)	I1−La2−I1	165.6(1)
La2−$I2^{a-i}$		3.435(5)	I2−La2−I2	166.6(1)

[a] Split position.

Structure. The presence of the relatively large host atoms La (or Pr), iodine, and interstitial Os together with the relatively small counterion K results in a new structure type with an unusual $R_6(Z)I_{14}$ network. α-$K_4La_6I_{14}Os$ and $K_4Pr_6I_{14}Os$ are isostructural and crystallize in the tetragonal space group $P4/mnc$ in the form of black, platelike crystals. Figures 1 and 2 show [100] and [001] views of the cluster framework in α-$K_4La_6I_{14}Os$. One significant feature is the high symmetry of the La_6 cluster, which is defined by two crystallographically distinct metal atoms and an Os atom that lies on an inversion center (4/*m*) (Figure 1). The apical La1 atoms lie on a 4-fold axis along $\vec{c}$, and the equatorial La2 atoms, on the mirror perpendicular to $\vec{c}$. The La−La distances, La1−La2 = 4.041(4) and La2−La2 = 4.045(4) Å, and the corresponding d(La−Os) (Table 3) describe a dimensionally ideal octahedron.

The 12 edges of the R_6Os clusters are bridged by two crystallographically distinct iodine atoms to form the well-known $R_6(Os)I_{12}$ unit with D_{4h} symmetry. The I1 atoms in each cluster cover the eight La1−La2 edges as I^i without bonding to adjacent clusters (Figure 1). Four I2 atoms with the functionality I^{i-a} bridge the four La2−La2 edges about the waist of the cluster and also form exo (I^{a-i}) bonds to four La2 atoms in adjacent clusters related by translation along a or b (Figure 2). These are naturally opposed by I2 atoms on the latter that bond to waist vertexes in the central cluster as I^{a-i}. Finally, each cluster has two axial I3 atoms bound to La1 that remain terminal I^a. Therefore, the interconnection pattern of the iodine atoms can be detailed as $(La_6Os)I^i{}_8I^{i-a}{}_{4/2}I^{a-i}{}_{4/2}I^a{}_2$. The La−$I^i$, La−$I^{i-a}$, and

(19) Guloy, A. M.; Corbett, J. D. *Inorg. Chem.* **1996**, *35*, 4669.
(20) (a) Whangbo, M.-H.; Hoffmann, R. *J. Am. Chem. Soc.* **1978**, *100*, 6093. (b) Ammeter, J. H.; Bürgi, H.-B.; Thibeault, J.; Hoffmann, R. *J. Am. Chem. Soc.* **1978**, *100*, 3686.
(21) Zeng, C.; Hoffman, R. Unpublished results.
(22) Vela, A.; Gázquez, J. L. *J. Phys. Chem.* **1988**, *92*, 5688.
(23) Payne, M. W.; Ebihara, M.; Corbett, J. D. *Angew. Chem., Int. Ed. Engl.* **1991**, *30*, 856.
(24) Payne, M. W.; Dorhout, P. K.; Corbett, J. D. *Inorg. Chem.* **1991**, *30*, 1467, 3112.

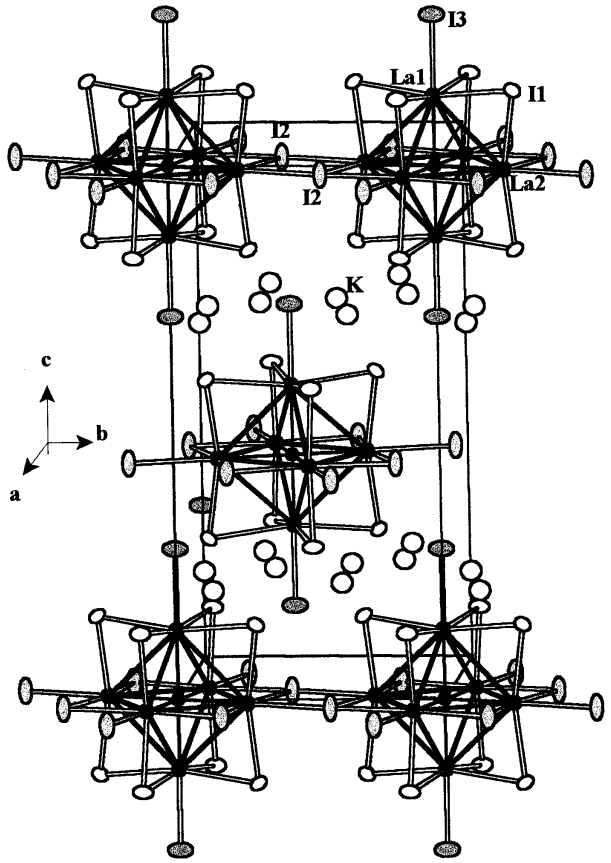

Figure 1. ~[100] view of the contents of the front of the unit cell of α-$K_4La_6I_{14}Os$ with atom labels. Inner iodine I^i, bridging I^{i-a} (I2), and K(split) are drawn with open (90%) ellipsoids, while I^a (I3) atoms have gray ellipsoids, and La and Os are black. The clusters are bridged into infinite planar nets generated by the translation $^1/_2$, $^1/_2$, $^1/_2$.

La−I^a separations are highly regular (3.26−3.31 Å), and the outer or exo La2−$I2^{a-i}$ bonds are longer (3.44 Å), as customary. The La2 and I2 atom arrangements on the mirror plane create a continuous planar network, as shown in Figure 2 in the [001] projection (without I^i) and in a perspective view. At the same time, the structure keeps all I···I contacts ≥4.39 Å, i.e., well above ~4.00 Å, where substantial matrix effects begin. A similar i−a, a−i connectivity of four clusters is found in the $R_6X_{10}Z$[25] structure type, but there the pairs of cluster connections are cis and orthogonal to each other.

The present $R_6(Os)I_{14}$ structural network is a notable contrast to the well-known Nb_6Cl_{14}, ANb_6Cl_{14}, and over 40 zirconium halide cluster systems with a wide range of interstitials, all with the same Nb_6Cl_{14}-type linkage.[1,26,27] These clusters are all interbonded by two trans X^{i-a} and four X^{a-a} functions to produce a unique three-dimensional network $(M_6Z)X^i{}_{10}$-$X^{i-a}{}_{2/2}X^{a-i}{}_{2/2}X^{a-a}{}_{4/2}$. A single alkali-metal cation per cluster may occupy one of two different sites depending on its size.[28,29] The present $K_4R_6I_{14}Os$ is to date the halogen-richest among all rare-earth-metal cluster halides. In addition, each cluster therein contains just 16 skeletal electrons (4·1 + 6·3 − 14 + 8), not the 18-e^- optimum.[27] The need to accommodate four extra cations per cluster, forced by the choice of Os for Z, is presumably a driving force for a different structure, while that for any compound with 18-e^- R_6Os clusters, six cations, and the same or other halide interconnections must be unstable. The undistorted clusters in $K_4La_6I_{14}Os$ and the reasons therefore appear to be very significant.

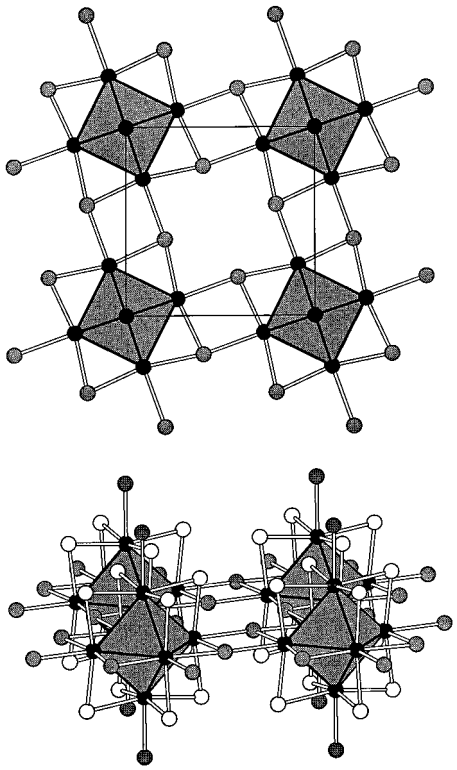

Figure 2. Views of the interbridged layers in α-$K_4La_6I_{14}Os$, with bridging I^{i-a} atoms shaded. Top: along [001], without K, I^i, and I^a atoms. Bottom: from the side, without K.

The cluster array therein contains two types of voids among the halide atoms that could host countercations, 8*g* at ~0.339, 0.839, 0.25 and 2*a* at $^1/_2$, $^1/_2$, $^1/_2$. However, only the former is occupied by potassium because the radius of the latter is much greater, 4.75 Å vs $\bar{d}_{obs}$ = 3.54 Å. The 8*g* cavity about K is oblong in terms of iodine neighbors, and the real disposition affords a sizable elongation of the K ellipsoid when refined as a single atom, more than 10 times those of other atoms. The position refines much better as two 50% K sites 0.90 Å apart (47(1)% occupancy each), a disorder that is clearly intrinsic rather than the result of the application of too-high a symmetry or twinning (see Experimental Section). There are two $I3^a$ at the ends and four $I1^i$ atoms around the waist of the cavity, and this provides reasonable bonding only when the cation is displaced to be in close contact with I3 at one end or the other (Supporting Information). Many examples are known among other quaternary cluster halides in which cations in poorly defined sites of low symmetry largely fulfill only charge compensation roles.[1,4,30] The present is one of the less extreme. The average K−I distance to five neighbors, 3.54 Å, is the same as the sum of crystal radii (CN6).[31] The −100 °C structure is basically the same but with smaller ellipsoids.

Properties. The high symmetry of the clusters and the linkages found in this structure are highly unusual, particularly when coupled with the absence of the tetragonal compression that is observed for many other 16-e^- clusters (to apparently yield $e_u{}^4$ from $t_{1u}{}^4$; below). One attractive explanation is that electrons in the nominal cluster HOMO $t_{1u}{}^4$ are delocalized. A

(25) Hughbanks, T.; Corbett, J. D. *Inorg. Chem.* **1989**, *28*, 631.
(26) Smith, J. D.; Corbett, J. D. *J. Am. Chem. Soc.* **1986**, *108*, 1927.
(27) Hughbanks, T.; Rosenthal, G.; Corbett, J. D. *J. Am. Chem. Soc.* **1988**, *110*, 1511.
(28) Zhang, J.; Corbett, J. D. *J. Solid State Chem.* **1994**, *109*, 265.
(29) Qi, R.-Y.; Corbett, J. D. *J. Solid State Chem.* **1998**, *139*, 85.
(30) Ziebarth, R.; Corbett, J. D. *Acc. Chem. Res.* **1989**, *22*, 256.
(31) Shannon, R. D. *Acta Crystallogr.* **1976**, *A32*, 751.

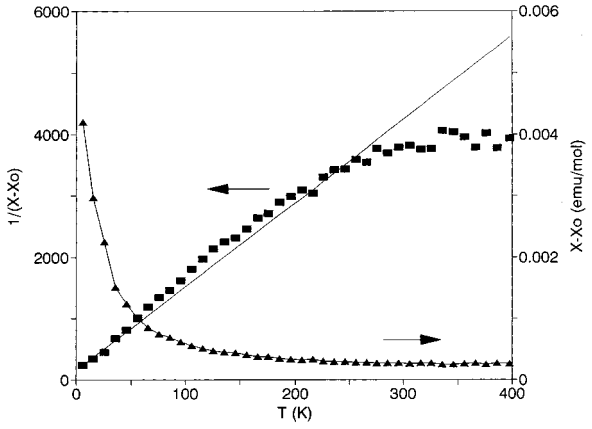

Figure 3. Magnetic susceptibilities $\chi - \chi_0$ (right) and $(\chi - \chi_0)^{-1}$ (left) as functions of temperature (K) for α-$K_4La_6(Os)I_{14}$ (3 T). The nonlinear fitting parameters refined for the entire range (the line drawn) are $\chi_0 = 3.50 \times 10^{-4}$ emu·mol^{-1}, $\Theta = -11$ K, $C = 7.34 \times 10^{-2}$, and $\mu_{eff} = 0.77\ \mu_B$.

metallic behavior in such a case would be a first among phases containing only isolated (noncondensed) halide clusters. Measurements of the resistivities of two different samples gave surprisingly low and substantially temperature-independent resistivities of ~120 and ~240 μΩ·cm, i.e., of a poor metal. The former data set, more consistent over a longer temperature range, is shown in the Supporting Information. These of course are upper limits for a powdered, supposedly 2D conductor. This behavior is far different from that of other noncondensed cluster halide systems which have always appeared to be insulators or very poor semiconductors. (Of course, only a few have been examined quantitatively because of the lack of other evidence for something unusual.) The one possible exception is $La_{12}I_{17}Fe_2$, a tightly interbridged, low-symmetry cluster network, for which a sample resistivity of ~350 μΩ·cm was considered a lower limit because of its 10% content of metallic LaI_2. There is one unpaired electron per formula unit (two clusters) in this case, and an observed moment of 1.11 μ_B was reasonable but not very informative.[32]

Magnetic susceptibility data measured for six samples from four different syntheses of α-$K_4La_6I_{14}Os$ were quite consistent and were not those of either a classical system or one troubled by varying impurities. A typical result is shown in Figure 3, and two others are contained in the Supporting Information. Fits of all of the data sets between 6 and either 300 or 400 K to the nonlinear expression $(\chi_M - \chi_0)^{-1} = (T - \Theta)/C$ gave moments of 0.6−0.8 μ_B, $-25 \le \Theta \le -6$ K, and χ_0 values around $(3.5-7.5) \times 10^{-4}$ emu mol^{-1}. It is especially noteworthy that the linear fittings are really satisfactory only from ~30 to about 200−300 K and that χ (and $(\chi - \chi_0)^{-1}$) becomes substantially constant at higher temperatures. All samples showed this characteristic. We show the general overall fits to make clear that the turnovers in $(\chi - \chi_0)^{-1}$ are not artifacts of the values of χ_0 or the temperature region of the fits. The presumed van Vleck TIP values of χ_0 are very typical of those measured for a variety of nonmagnetic cluster halide systems of similar constitution.[7,33] (The χ_0 values are 2−3 times the inferred TIP Pauli term at and about room temperature; below.)

The correlation of these observations with cluster distortion is significant. Eighteen electrons is well-known to be optimal for octahedral 6−12 clusters centered by transition elements, corresponding to the R−Z bonding $a_{1g}^2\ t_{2g}^6$, the nonbonding e_g^4 on Z, and the R−R bonding HOMO t_{1u}^6.[8] Accordingly, many 16-electron clusters with potential t_{1u}^4 HOMOs have been found to exhibit appreciable tetragonal distortions, namely $Y_6I_{10}Ru$ (by 0.21 Å in Δ*d*(Y−Ru), 50% of the compression),[25] $K_2La_6I_{12}Os$ (0.25 Å),[7] and $Pr_6Br_{10}Ru$ (0.28 Å),[34] as well as 0.16 Å for eight of nine independent clusters in the related superstructure of $La_{48}Br_{81}Os_6$ (0.16 Å).[35] A few other compounds with 16-e$^-$ clusters show relatively smaller distortions, e.g. $Y_6I_{10}Os$ (0.09 Å)[36] and two with low-symmetry clusters or bridging, β-$K_4La_6I_{14}Os$ (~0.11 Å elongation)[12] and $CsLa_6I_{10}Mn$ (0.05 Å).[4] The natures of the bridging halogen network in the last two seem to play a role in limiting or restricting the degrees of distortions. However, the means of cation accommodation and the interactions between the layers in α-$K_4La_6I_{14}Os$ (Figure 1) in no way afford a reasonable explanation for the lack of a tetragonal compression of these clusters in terms of an insurmountable elastic energy of the system. Indeed, a tetragonal compression would appear to be notably less restrained here than in other heavily interbridged cases. The answer appears to be found in an extension of our bonding concepts to longer range properties and bands (below).

A good general correlation is found between these distortions and the inherent magnetic properties, where known. Both $K_2La_6I_{12}Os$ and β-$K_4La_6I_{14}Os$ exhibit only temperature-independent (presumed van Vleck) paramagnetism, suggesting closed ground states. On the other hand, nonlinear fitting of magnetic data for the least distorted $CsLa_6I_{10}Mn$ (above) shows a nearly ideal moment for two unpaired electrons, 2.9 μ_B over ~125−300 K, and similarly for the isostructural 17-e$^-$ $CsLa_6I_{10}Fe$ for one electron (1.4 μ_B) over 150−300 K. The present, virtually undistorted α-$K_4La_6I_{14}Os$ is a typical paramagnet at lower temperatures, but with μ_{eff} values near only 0.7 μ_B. A further antiferromagnetic-like coupling occurs but only near 30 K, despite the appreciable electronic conductivity. Most importantly, the temperature dependence of the localized paramagnetic spins effectively disappears above 270−300 K to yield a spin-paired system with what we interpret to be the Pauli-like paramagnetism of delocalized conduction electrons. More interpretation will follow the supportive findings from band calculations.

Calculations. As expected, EHMO calculations on a single cluster $(La_6I_{14}Os)I_4^{8-}$ with the observed dimensions predict very little deviation (~0.02 eV) from a degenerate t_{1u}^4 system, consistent with the cluster dimensions along with some tetragonality induced by the different bridging iodine functions. Earlier extended Hückel MO calculations of the same type for the tetragonally compressed cluster and the surrounding halogens in $Y_6I_{10}Ru$[25] showed that splitting of the t_{1u}^4 HOMO into a two-below-one pattern resulted largely from interactions between Y 4d orbitals, with very little participation of Ru 5p. Similar EHMO calculations on the isolated clusters in the TIP examples $K_2La_6I_{12}Os$ and β-$K_4La_6I_{14}Os$ forecasted only small splittings of the nominal t_{1u} HOMO (0.14 eV in the former, 0.07 eV in the latter but without allowance for the very asymmetric iodine bridging) for compounds that are experimentally closed shell. The converse, very little splitting and paramagnetism, apply to the two $CsLa_6I_{10}Z$ systems with small to zero distortions (above).

A partial band diagram according to a 2D EHTB (tight binding) calculation for the anion structure in solid α-$K_4La_6I_{14}$-

(32) Lulei, M.; Martin, J. D.; Corbett, J. D. *J. Solid State Chem.* **1996**, *125*, 249.
(33) Steinwand, S. J.; Corbett, J. D. *Inorg. Chem.* **1996**, *35*, 7056.
(34) Llusar, R.; Corbett, J. D. *Inorg. Chem.* **1994**, *33*, 849.
(35) Hong, S.-T.; Hoistad, L. M.; Corbett, J. D. *Inorg. Chem.*, submitted for publication.
(36) Payne, M. W.; Corbett, J. D. *Inorg. Chem.* **1990**, *29*, 2246.

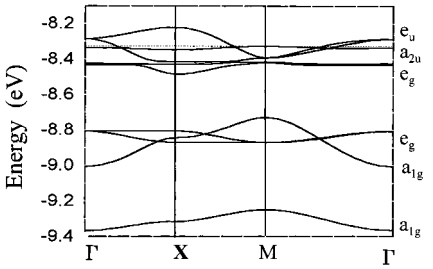

Figure 4. EHTB results for the 2D bands in the extended solid $La_6I_{14}Os^{4-}$ ($\mathbf{X} = a^*/2$, $\mathbf{M} = a^*/2, b^*/2$).

Os is shown in Figure 4 for the region around E_F. A significant dispersion of about 0.27 eV is achieved in the e_u subband at **X** ($a^*/2$), that is, in reciprocal space in the directions of the *a* and *b* crystal axes, vs only a ~0.05 eV separation of the a_{2u} and e_u components at **Γ** and a generally small dispersion of the interstitial-based e_g^4. The 0.27 eV dispersion is about twice what would be found for a comparable 1D chain and much greater than the splitting found for the isolated cluster. The intercluster communication takes place particularly via La $d_{x^2-y^2}$ and iodine p orbitals in the e_u band, whereas the bridging iodines in the a_{2u} representation are only π^* in the I^{a-i} function, so that band is quite flat. The e_u subband illustrated might still be viewed by some as relatively narrow, since the general restrictions and problems of bandwidth vs local on-site repulsions in the Hubbard sense presumably apply.[37] However, the local repulsions are likely to be smaller here, as they pertain to localization not on atomic sites but in cluster MO's.

The Mott−Hubbard type localization inferred at lower temperatures occurs when kT is no longer sufficient to overcome on-site repulsions and the pairing energy for the conduction electrons exceeds that of the bandwidth. Furthermore, the lowest states formed upon localization of the electrons in the t_{1u}-type "conduction bands" (e_u and a_{2u}) may be occupied by paired electrons in a different cell, leaving only a fraction of the electrons unpaired in some magnetic states near the Fermi level. It is thus reasonable to propose that the small remaining moment of 0.7 μ_B per formula unit (corresponding to ~0.2 e^- (spin only)) represents the small unpaired component of the localized Mott−Hubbard system. This corresponds to about 1 unpaired electron per four or five clusters. The absence of significant exchange coupling of these spins until 30 K is further consistent with the diluteness of the spins. Were the e_g^4 level to lie nearer E_F (Figure 4), μ_{eff} might instead reflect a small number of localized vacancies in these states, which are nominally on the osmium interstitial and well removed from the conduction band derived from lanthanum and iodine states. But such an extreme is probably not necessary for understanding the behavior.

Conclusions. The syntheses of α-$K_4R_6I_{14}Os$ (R = La, Pr) with their unusual cluster connectivities and all the delocalization implications thereof clearly demonstrate how the introduction of alkali metals can result in the formation of more open and less bridged structures. In the present case, this amounts to a formal addition of 4 KI to the heavily condensed $Y_6I_{10}Ru$-type structure already known for $Pr_6I_{10}Os$.[34] The more versatile and interesting of these quaternary phases are those stabilized by transition-metal atoms rather than by main-group nonmetals or metalloids, perhaps because the heavier members expand the clusters and lessen the energy differences among levels in the neighborhood of the HOMO. This is immediately evident in the greater variety of Z that can be incorporated or, in another sense, the expanded range of skeletal electron counts that is possible in some structure types, 16−20.[36] The present compound is immediately unusual because it lacks the tetragonal cluster distortions and the diamagnetism that are customarily associated with 16-e^- cluster units, particularly in the absence of any clear structural restraint. Instead, the compound exhibits a small paramagnetism that disappears near room temperature, not the paramagnetic "t_{1u}^4" result of an undistorted cluster. A low resistivity is also found, largely unprecedented among halogen-interbridged cluster compounds. Finally, the 2D band calculation makes clear the increased dispersion and delocalization that can be achieved in this 2D-planar net of iodine-bridged clusters, which was the first unexpected feature of this new cluster structure.

Acknowledgment. We thank Jerome Ostenson for the magnetic data and calculations, Paul Maggard for the resistivity measurements, and Gordie Miller and Paul Canfield for advice. We also thank Kenneth Poeppelmeier for reminding us over the years that such delocalization characteristics might be found in a system built of nominally isolated clusters. This research was supported by the National Science Foundation, Solid State Chemistry, via Grants DMR-9510278 and -9809850 and was carried out in the facilities of Ames Laboratory—DOE.

Supporting Information Available: Tables of additional refinement information and anisotropic displacement parameters for $K_4La_6I_{14}Os$ at room temperature as well as all of the structural results for $K_4Pr_6I_{14}Os$ and for $K_4La_6I_{14}Os$ at −100 °C and illustrations of the cation site in, plus the conductivity results and two more sets of magnetic data for, $K_4La_6I_{14}Os$. This material is available free of charge via the Internet at http://pubs.acs.org.

IC990638F

(37) Cox, P. A. *The Electronic Structure and Chemistry of Solids*; Oxford University Press: Oxford, U.K., 1987; Chapter 5.